Available online at www.sciencedirect.com
ScienceDirect
Materials Science and Engineering C 28 (2008) 731–738
MATERIALS SCIENCE & ENGINEERING C
www.elsevier.com/locate/msec

Design of new electropolymerized polypyrrole films of polyfluorinated Zn(II) and Mn(III) porphyrins: Towards electrochemical sensors

Maria A. Carvalho de Medeiros [a], Karine Gorgy [b], Alain Deronzier [b], Serge Cosnier [b,*]

[a] Centro Superior de Educação Tecnológica (CESET) - Universidade Estadual de Campinas (UNICAMP) - Campus de Limeira, Rua Pachoal Marmo, 1888 - Cx. Postal 456 - Limeira - SP, CEP 13484-420, Brazil
[b] Département de Chimie Moléculaire, UMR - 5250, ICMG FR - 2607, CNRS, Université Joseph Fourier BP 53, 38041 Grenoble Cedex 9, France

Available online 12 October 2007

Abstract

New Zn (II) and Mn (III) porphyrins functionalized by one and four electropolymerizable pyrrole groups respectively have been synthesized and their electrochemical behavior was characterized in acetonitrile electrolyte. The electrooxidation of these metallopolyfluoroporphyrins has allowed the formation of N-substituted polypyrrole films. The latter exhibit electrochemical behaviors identical to those of the corresponding monomers combined with the conventional electroactivity of the polypyrrole skeleton. Moreover, the potential electrocatalytic properties of Mn (III)-based polypyrrole films in the presence of molecular oxygen and benzoic anhydride have been illustrated by cyclic voltammetry in organic solution. In addition, preliminary experiments have also demonstrated the potentialities of such polymeric films for the electrochemical detection of H_2O_2 in aqueous media.

Keywords: Electropolymerization, Polypyrrole, Metallofluoroporphyrin, Zn(II) polyfluoroporphyrin, Mn(III) polyfluoroporphyrin

1. Introduction

For the last four decades, there has been a growing interest in the design of biosensors as portable and economical tools in analytical chemistry. Among the various combinations of biomolecule-transducer, electrochemical biosensors based on the molecular recognition properties of enzymes, represent the most common category [1]. However, most of these analytical devices suffer from poor operational and storage stabilities due to the fragility of the protein structure. In particular, inhibition processes or denaturation due to protein unfolding, high temperatures or harsh chemical conditions may rapidly annihilate the activity of immobilized enzymes.

An attractive strategy consists of replacing the proteins by electroactive synthetic complexes that mimic the structure and/or the activity of the prosthetic groups of enzymes on an electrode surface. These immobilized biomimetic compounds should be more stable than enzymes in aqueous or organic media, particularly in extreme pH or temperature. Furthermore, the immobilization of such model systems on electrode is a convenient way for understanding the mechanism of enzyme-catalyzed transformations. Since metalloporphyrins, chlorins, bacteriochlorins, isobacteriochlorins, and corrins play important roles in many vital biological processes implying an electron transfer [2,3], the design of electrodes modified by coating materials containing porphyrinic structures has been subject of an intense effort last three decades. In particular synthetic metalloporphyrins appear as one of the most promising classes of enzyme analogs, owing to their functions as redox mediators, catalysts or selective complexing centers via axial ligation reactions. Moreover, the direct electron exchange between these various metalloporphyrins and electrodes constitutes an elegant approach to study enzyme reactions by excluding the requirement of a chemical redox mediator to shuttle electrons between enzyme and electrode. Among the conventional methods of metalloporphyrin deposition, their immobilization as electropolymerized films has been widely used [4–15]. The main advantage of the electrochemical polymerization lies in the non-manual electrochemical addressing of polymers and hence in the reproducibility of the polymer formation and the precision for the functionalization of conductive surfaces

* Corresponding author. Tel.: +33 4 76 51 49 98; fax: +33 4 76 51 42 67.
E-mail address: Serge.Cosnier@ujf-grenoble.fr (S. Cosnier).

0928-4931/$ - see front matter © 2007 Elsevier B.V. All rights reserved.
doi:10.1016/j.msec.2007.10.016

whatever their size and geometry are. Furthermore, the electropolymerization of metalloporphyrins provides densely packed monomer layers that facilitate the electron hopping process between metalloporphyrin sites and allows the formation of films of controlled thickness. Moreover, the polymeric films are stable in aqueous and organic solvents allowing thus the transfer of biomimetic activities in non-aqueous media. Among the conducting polymers, functionalized polypyrroles play the leading role as polymeric skeleton for the elaboration of electropolymerized metalloporphyrin films.With the aim to design electropolymerized metalloporphyrin films exhibiting an enhanced stability, the substitution of the metalloporphyrin macrocycle by electron-withdrawing pentafluorophenyl groups was previously reported for a series nickel (II) tetrakis (polyfluorophenyl) porphyrins functionalized by pyrrole groups [5]. Numerous studies have indeed demonstrated that the stability of the metalloporphyrins as catalyst for alkane hydroxylation or olefin epoxidation was markedly improved if the macrocycle is polyhalogenated [16–19].

In that context, we describe here the electrochemical characterization of new Zn (II) and Mn (III) tetrakis(pentafluorophenyl)porphyrins substituted by electropolymerizable pyrrole groups (Fig. 1) and their electropolymerization. Their electro-oxidation in organic solvent has allowed the formation of stable conducting polypyrrole films exhibiting electrochemical behaviors identical to those of the corresponding monomers as well as that due to the polypyrrole matrix. In addition, the potential electrocatalytic properties of Mn (III)-based polypyrrole films in the presence of oxygen and benzoic anhydride or H_2O_2 were evaluated in organic and aqueous media.

2. Experimental part

2.1. Reagents

Tetrachloro-1,4-benzoquinone (para-chloranil), 2,3-dichloro-5,6-dicyano-1,4-benzoquinone (DDQ), pentafluorobenzaldehyde, boron trifluoride etherate (BF_3·Et_2O), $ZnCl_2$, $MnCl_2$, cyclohexane, DMF, 3-amino-1-propanol, 2,5-dimethoxytetrahydrofuran, 1-methylimidazole were used as received from Aldrich. Acetonitrile (CH_3CN, Rathburn, HPLC grade) was used as received and stored under an argon atmosphere in a glove box. Dichloromethane (CH_2Cl_2) was dried over neutral alumina for at least 6 days. Tetra-n-butylammonium perchlorate (TBAP, Fluka) was recrystallised from ethyl acetate+ cyclohexane and dried under vacuum at 80 °C for 3 days. Tetrahydrofuran (THF, analytical grade) were purchased from Riedel-de Haën and distilled under an argon atmosphere.

1-(3-hydroxypropyl)pyrrole was synthesized as previously reported by Carpio and coworkers [20].

H_2TPFP: 5, 10, 15, 20-tetrakis(pentafluorophenylporphyrin was synthesized and purified as previously described [5]. The H_2TPFP was characterized by ^{19}F NMR spectroscopy (Table 1). UV-visible data [λ_{max}, nm (10^{-4} ε M^{-1} cm^{-1})], CH_2Cl_2: 410 (26.2), 504 (18.3), 582 (0.56), 636 (0.09). IR (KBr): 1064, 1080 cm^{-1}.

ZnTPFP: The zinc(II) [5, 10, 15, 20-tetrakis(pentafluorophenyl)porphyrin] was prepared following the method reported by Kadish [21] and characterized by ^{19}F NMR spectroscopy (Table 1). Mass spectral data ($C_{44}H_8F_{20}N_4Zn$): calculated MW 1037.92; m/z of the parent peak at 1036. UV–visible data [λ_{max}, nm (10^{-4} ε M^{-1} cm^{-1})], CH_2Cl_2: 412 (47.2), 542 (2.04), 578 (0.52). IR (KBr): 1064, 1080 cm^{-1}.

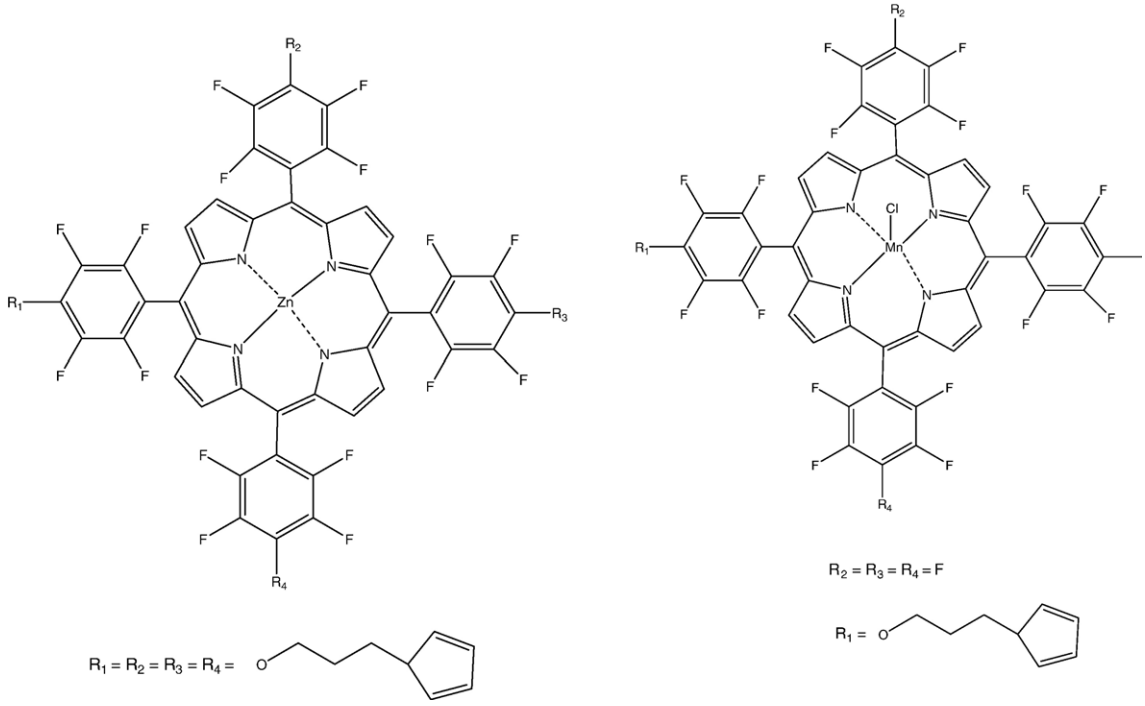

Fig. 1. Structure of the momomers ZnTPFPy (II) and Mn (III) MnTPFPy tetrakis(pentafluorophenyl)porphyrins.

Table 1
^{19}F NMR data recorded in CDCl3 [a]

Compound	^{19}F NMR [b]				
	o-F′	o-F″	p-F	m-F′	m-F″
H_2TPFP	−136.95(m)	–	−151.67(t)	−161.77(m)	–
ZnTPFP	−137.40(m)	–	−152.50(t)	−162.30(m)	–
ZnTPFPy	–	−138.96(t)	–	–	−157.86(m)
MnTPFPCl	−149.81(1s)	–	−156.97(1s)	−158.08(1s)	–
MNTPFPPy	−156.00(1s)	−158.1(1s)	−158.58(1s)	−159.78(1s)	−160.19(1s)

[a] In ppm, ^{19}F NMR vs $CFCl_3$; d = doublet; t = triplet; m = multiplet.
[b] F′ are in unsubstituted pentafluorophenyl groups, and F″ are in substituted pentafluorophenyl groups.

ZnTPFPPy: The zinc(II) complex functionalized by four 3-(pyrrol-1-yl)propyloxy groups via the substitution of the para-F atoms of ZnTPFP was synthesized by the following procedure: 1-(3hydroxypropyl)pyrrole (1.7×10^{-3} mol) was refluxed in THF (10 ml) with Na (1.7×10^{-2} mol) for 6 h under an argon atmosphere. After cooling to 25 °C, ZnTPFP (3.4×10^{-4} mol in 10 ml of THF) was added to the preceding mixture and refluxed for 24 h under an argon atmosphere. The solvent was evaporated and then the product was washed with H_2O and extracted with CH_2Cl_2. The organic phase was dried over anhydrous Na_2SO_4. After filtration and evaporation of the solvent under reduced pressure, the resulting red product was purified by chromatography (silica gel column eluted with a 2:1 cyclohexane/dichloromethane). ZnTPFPPy (80% yield) was characterized by ^{19}F NMR spectroscopy (Table 1). Mass spectral data ($C_{72}H_{48}F_{16}N_8O_4Zn$): calculated MW 1456.28; m/z from the parent peak at 1456. UV–visible data [λ_{max}, nm (10^{-4} ε M^{-1} cm^{-})], CH_2Cl_2: 414 (42.9), 548 (1.86), 628 (0.47). IR (KBr): 1066, 1082, 1281 cm^{-1}.

MnTPFCl: Mn (III) [5, 10, 20-tetrakis(pentafluorophenyl) porphyrin]chloride was prepared according to the general procedure described for Ni (II) tetrakis(polyfluorophenyl) porphyrin [5].

H_2TPFP (5.13×10^{-5} mol) was dissolved in anhydrous DMF (50 mL). Anhydrous manganese (II) chloride (4.0×10^{-4}) was added and the mixture was refluxed under argon for 5 h. The solvent was evaporated and then the product was washed with water and extracted with CH_2Cl_2. The organic phase was dried over anhydrous Na_2SO_4, concentrated and filtered and then the solvent was evaporated. The residue was then chromatographed on silica gel column eluting with CH_2Cl_2/methanol (95/5) to give Mn TPFPCl as a brown solid (40% yield). The manganese (III) complex was characterized by ^{19} F NMR spectroscopy (Table 1). Mass spectral data ($C_{44}H_8F_{20}N_4MnCl$): calculated MW 1062; m/z of the parent peak at m/z = 1027 ($C_{44}H_8F_{20}N_4Mn^{+}$). UV–visible data [λ_{max}, nm], CH_3CN: 360, 470, 566.

MnTPFPPy: Mn (III) [5, 10, 20-tetrakis(pentafluorophenyl) porphyrin]chloride functionalized by one 3-(pyrrol-1-yl)propyloxy group via the substitution of one para-F atom of MnTPFPCl was synthesized according to the general procedure described for Zn TPFP. A MnTPFPCl solution (4.42×10^{-5} mol) in THF (10 mL) was mixed with one equivalent of the activated pyrrole derivative and the reaction mixture was mixed with one equivalent of the activated pyrrole derivative and the reaction mixture was refluxed for 24 h under an argon atmosphere. The solvent was evaporated and then the product was washed with water and extracted with CH_2Cl_2. The organic phase was dried over anhydrous Na_2SO_4, filtered, concentrated and then the residue was chromatographed on silica gel column eluted with dichloromethane/methanol (95/5). MnTPFPPy (40% yield) was characterized by ^{19}F NMR spectroscopy (Table 1). Mass spectral data ($MnC_{51}H_{18}F_{19}N_5OCl$): calculated MW 1168 ; m/z from the parent peak at 1132 ($MnC_{51}H_{18}F_{19}N_5O^{+}$). UV–visible data [$\lambda_{max}$, nm], CH_3CN: 363, 471, 569.

2.2. Apparatus

All electrochemical experiments were performed using a Priceton Applied Research model 173 (PAR 173) equipped with a model 179 digital coulometer and a model 175 universal programmer in conjunction with a Sefram TGM 164, X–Y/t recorder.

The electrochemical characterization of the monomers, their electrochemical polymerization and the characterization of the resulting modified electrodes were run at room temperature under an argon atmosphere using a conventional three-electrode cell.

An Ag/10 mM Ag^{+} in CH_3CN+0.1 M TBAP electrolyte electrode was used as the reference in CH_3CN. The electrochemical experiments in CH_2Cl_2 were performed with a Ag/AgCl/LiCl salt in EtOH electrode as reference electrode. A Pt wire, placed in a separate compartment containing the supporting electrolyte, was used as a counter electrode. All the potentials are reported to the Ag/10 mM Ag^{+} reference electrode. The working electrodes were glassy carbon or platinum disks (diameter respectively 3 or 5 mm). Both were systematically polished with 1 μm diamond paste (MECAPREX Press PM).

In aqueous solutions, all the potentials are reported to Ag/AgCl/KCl sat electrode.

3. Results and discussion

3.1. Redox behavior of the ZnTPFPPy and MnTPFPPy monomers

The electrochemical behavior of ZnTPFPPy and MnTPFPPy was investigated by cyclic voltammetry at a glassy carbon electrode. Fig. 2A shows the cyclic voltammogram of ZnTPFPPy (2 mM) in CH_3CN+0.1 M TBAP. Upon reductive scanning the voltammogram presents two reversible peak systems at $E_{1/2}$ = −1.41 and −1.77 V, attributed to the two successive one-electron reduction of the porphyrin ring into its radical anion and dianion forms respectively. The potential values of these two redox processes are less negative than those (−1.58 and −1.98 V) previously reported for Zn (II) tetraphenylporphyrin illustrating the influence of the macrocycle substitution, namely the electron-withdrawing effect of the tetrafluorophenyl groups. It should be noted that the difference between the first and second reduction potential

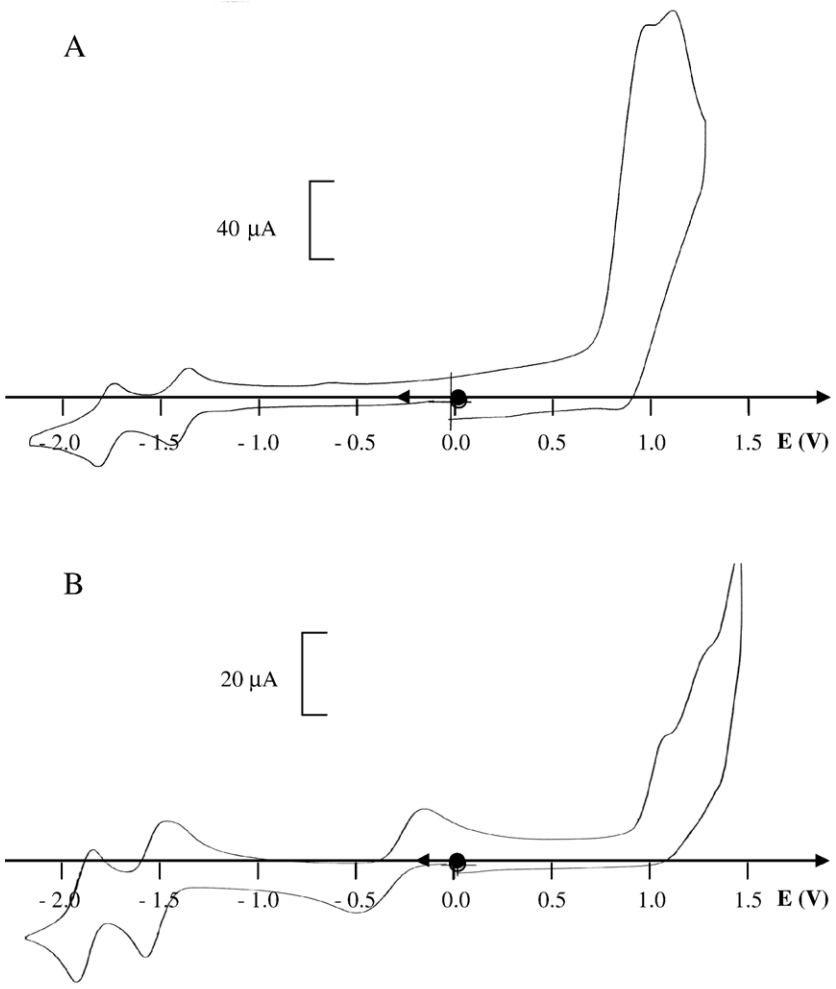

Fig. 2. Cyclic voltammograms recorded at a carbon electrode (5 mm disc) of 1 mM ZnTPFPyr (A) and MnTPFPyr (B) at a scan rate of 100 mV/s in CH_3CN+0.1 M TBAP. Potential measured vs Ag/Ag^+ 10 mM in CH_3CN+0.1 M TBAP.

values ($\Delta E_{1/2}$=0.36 V) is similar to the separation value ($\Delta E_{1/2}$=0.44±0.04V) already described for the two electron reduction of metalloporphyrin [22]. Upon oxidative scanning, the cyclic voltammogram of ZnTPFPPy exhibits two merged irreversible anodic peaks at 0.98 and 1.10 V. By analogy with the electrochemical behavior of a nickel (II) tetrakis (polyfluorophenyl) porphyrin [5], the first anodic peak was assigned to the mediated oxidation of the pyrrole groups by the electrogenerated radical cation form of the Zn porphyrin. The second peak was attributed to the dication formation of the porphyrin ring. The comparison of the intensity of the first irreversible anodic peak with that of the one-electron reduction of the macrocycle, is around 10. This ratio is in good accordance with the theoretical number of electrons involved in the oxidation of the macrocycle and four pyrrole groups, namely 10.32. In addition to the one-electron oxidation of the porphyrin, this value corresponds to the number of electrons involved in the electropolymerization of each pyrrole group (2 electrons $molecule^{-1}$) plus that for the electro-oxidation of the generated polypyrrolic chain (0.33 $electron\ molecule^{-1}$) [23].

Fig.2B shows the electrochemical behaviour of MnTPFPPy (2 mM) in CH_3CN+0.1 M TBAP at 0.1 V s^{-1}. Upon reductive scanning, the cyclic voltammogram exhibits a reversible peak

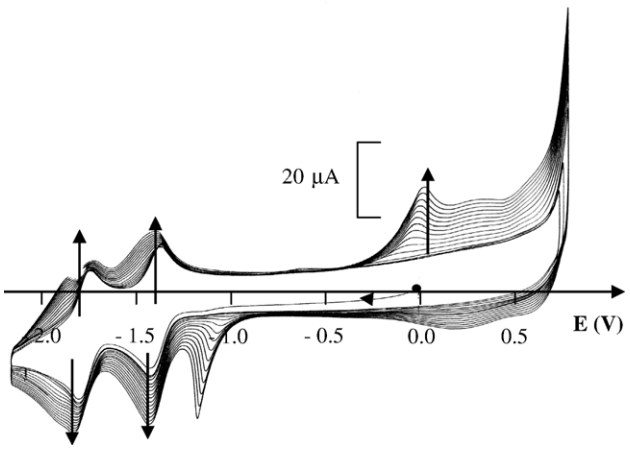

Fig. 3. Cyclic voltammograms recorded at a carbon electrode (5 mm disc) of 1 mM ZnTPPyr in CH_3CN+0.1 M TBAP between −2.16 V and +0.80 V; scan rate: 100 mV/s. Potential measured vs Ag/Ag^+ 10 mM in CH_3CN+0.1 M TBAP.

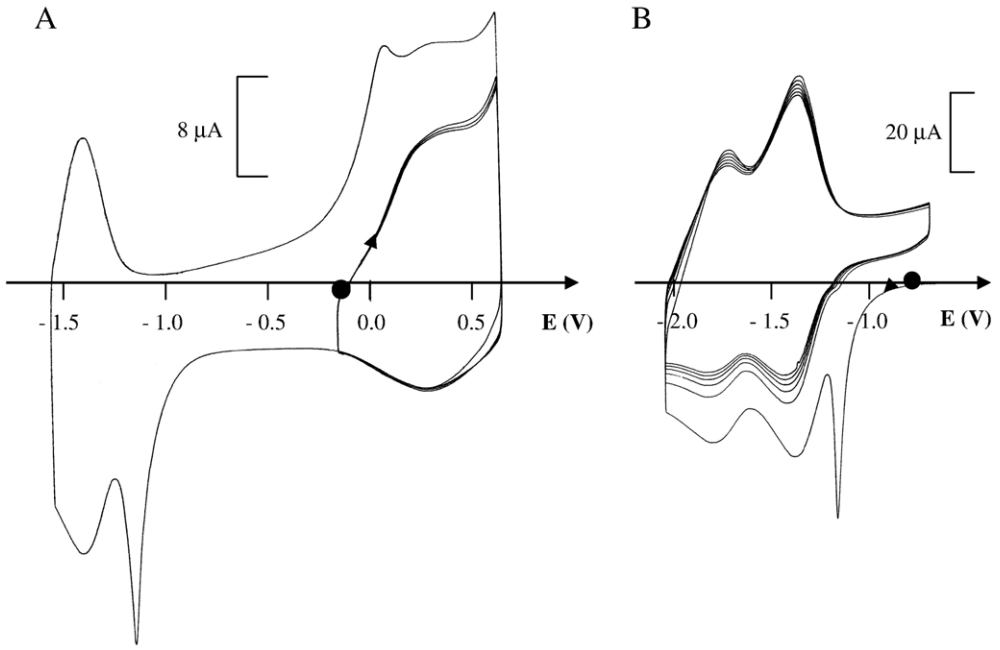

Fig. 4. Cyclic voltammograms recorded at a carbon electrode (5 mm disc) of poly[ZnTPPyr] transferred in a solution of CH_3CN+0.1 M TBAP free of monomer; scan rate: 100 mV/s. Potential measured vs Ag/Ag^+ 10 mM in CH_3CN+0.1 M TBAP. A: Scanning the positive region first, B: Scanning the negative region first.

system at −0.34 V corresponding to the Mn^{III}/Mn^{II} redox couple. The comparison with the electrochemical behavior of conventional or pyrrole-substituted Mn (III) tetraphenylporphyrins clearly indicates a marked positive shift of the Mn^{III}/Mn^{II} redox couple, namely −0.34 V instead of −0.58 V or −0.64 V [25,24]; This phenomenon illustrates the influence of the macrocycle halogenation. The reduction of the metal center was followed by two reversible peak systems due to the successive one-electron reduction of the porphyrin ring into its radical anion and dianions forms at −1.46 V and −1.87 V respectively. It should be noted that the difference between the first and the second reduction potentials ($\Delta E_{1/2}$=0.40 V) is similar to the separation value previously reported for the two electron reduction of ZnTPFPPyr. In the positive part, two merged irreversible anodic peaks appear at 1.00 V and 1.20 V assigned to the one-electron oxidation of MnTPFPy and the two-electron oxidation of the pyrrole group respectively.

3.2. Electrochemical generation and characterization of polypyrrole films of polyfluorinated Zn(II) and Mn(III) porphyrins

The electropolymerization properties of Zn and Mn porphyrins (2 mM) were investigated by cyclic voltammetry in CH_3CN+0.1 M TBAP. Repeatedly scanning the potential over the range −2.20 to +0.80 V for ZnTPFPPyr (Fig. 3) results in the appearance and the continuous growth of the reversible oxidation wave of the polypyrrolic film. In addition, a continuous increase in the height of the peak systems due to two successive one-electron reduction of the metalloporphyrin occurs in conjunction with the appearance and the increase of a characteristic cathodic pre-peak related to the polypyrrole

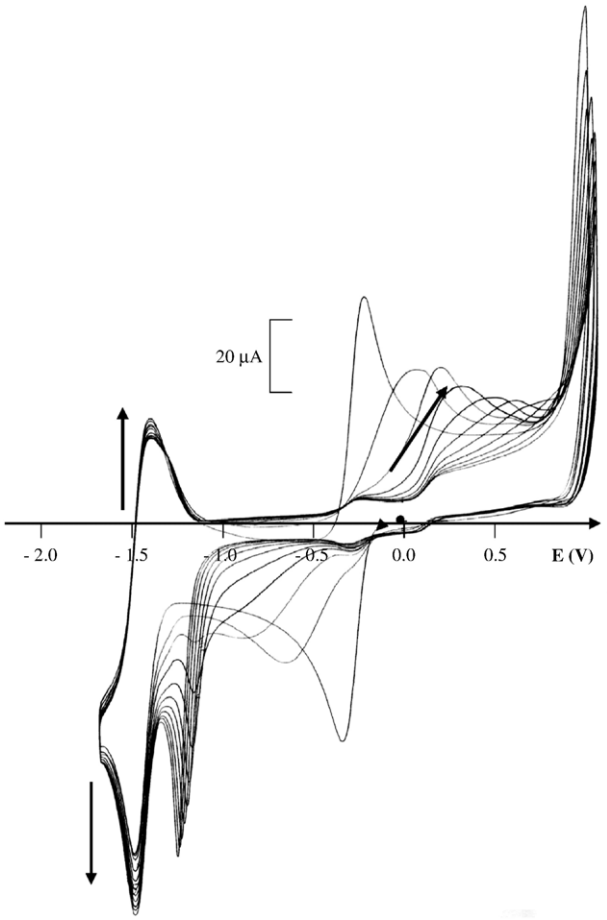

Fig. 5. Cyclic voltammograms recorded at a carbon electrode (5 mm disc) of 1 mM MnTPFPyr in CH_3CN+0.1 M TBAP between −1.70 V and 1.07 V; scan rate: 100 mV/s. Potential measured vs Ag/Ag^+ 10 mM in CH_3CN+0.1 M TBAP.

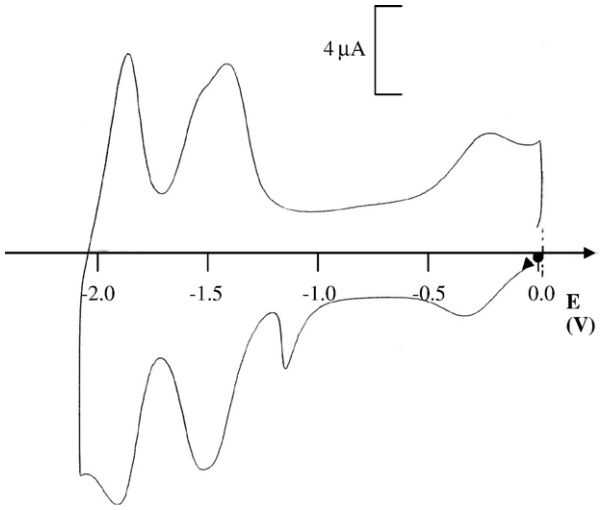

Fig. 6. Cyclic voltammogram recorded at a carbon electrode (5 mm disc) of poly [MnTPPyr] transferred in a solution of CH_3CN+0.1 M TBAP free of monomer in the negative region; scan rate: 100 mV/s. Potential measured vs Ag/Ag^+ 10 mM in CH_3CN+0.1 M TBAP.

skeleton [26]. This clearly indicates the formation of an electrogenerated film on the electrode surface as a consequence of the oxidation of the pyrrole groups. After a period of scanning (e.g. 12 cycles at 0.1 Vs^{-1}), the glassy carbon electrode was covered by a dark blue and adherent thin polymeric film of poly-(ZnTPFPPy). The latter was thoroughly rinsed and transferred into a CH_3CN+0.1 M TBAP solution free of monomer. The cyclic voltammogram scanning the potential over the range −1.60 to +0.60 V of the modified electrode clearly shows the reversible oxidation of the polypyrrole matrix ($E_{1/2}$=0.28 V with an anodic-cathodic peak separation, ΔE_p=0.06 V, v=0.1 Vs^{-1}) (Fig. 4A). In addition, the polypyrrolic film presents the regular electroactivity of the immobilized Zn (II) porphyrin as illustrated by the reversible peak system at −1.42 V. As previously described for other polypyrrole metalloporphyrin films [9], the pre-peak initiating the polypyrrole oxidation wave was totally vanished if the potential scanning was restricted to the potential range of the polypyrrole electroactivity (Fig. 4). In the same vein, the cyclic voltammogram shows an intense prepeak at the foot of the macrocycle reduction wave that disappears on the second scan if the potential scan range is restricted to the negative region. It should be noted that these prepeaks could be fully restored after a sweep in the positive or negative region for the cathodic or the anodic prepeak, respectively. The latter are a characteristic feature of the electrochemical behavior of the functionalized polypyrrole films and reflect their low conductivity compared to

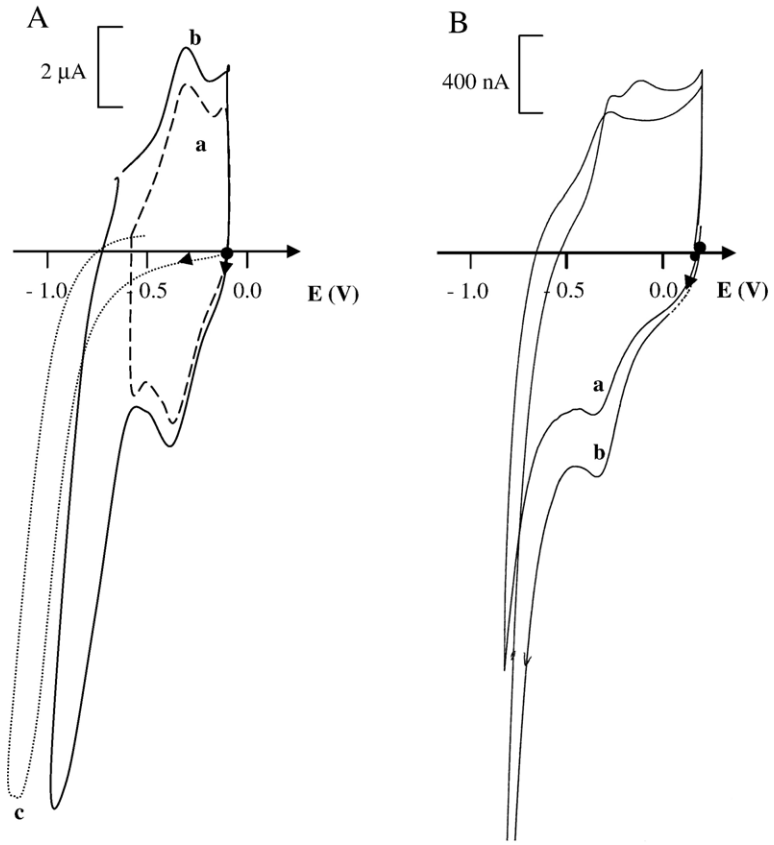

Fig. 7. (A) Cyclic voltammograms recorded in a solution of CH_2Cl_2+0.1 M TBAP of (a) a carbon modified electrode of poly[MnTPPyr] (5 mm disc) in presence of benzoic anhydre (10 mM) and 1-methylimidazole (5 mM) without O_2. Scan rate: 10 mV/s, (b) GC (5 mm disc) modified electrode of poly[MnTPPyr] (5 mm disc) in presence of benzoic anhydre (10 mM) and 1-methylimidazole (5 mM) in presence of O_2. Scan rate : 10 mV/s, (c) GC (5 mm disc) in presence of benzoic anhydre (10 mM) and 1-methylimidazole (5 mM) and O_2. Scan rate: 10 mV/s, (B) Cyclic voltammograms of poly[MnTPPyr] recorded in a solution of CH_2Cl_2+0.1 M TBAP in presence of 1-methylimidazole (5 mM) and O_2. Scan rate: 10 mV/s, (a) without benzoic anhydre, (b) in presence of benzoic anhydre (10 mM).

redox systems immobilized on these films [13,26]. If the potential scan range is extended to −2.2 V, the cyclic voltamogram presents an electrochemical behavior identical to that of the corresponding monomer, namely two reversible peak systems corresponding to the successive one-electron reduction of the macrocycle (Fig. 4B). The apparent surface coverage of poly (Zn TPFPPy) was estimated from the charge recorded under two different electrochemical systems: the one-electron reduction peak of Zn TPFPPy and the polypyrrole oxidation wave (each polymerized pyrrole group being oxidized by 0.33 electron). The amount of electropolymerized metalloporphyrin was evaluated from the latter signal by taking into account that theoretically four pyrrole units were polymerized for each porphyrinic monomer. The good accordance between the amounts of poly (Zn TPFPPy) (2.9 nmol cm^{-2} from the polypyrrolic backbone and 3.1 nmol cm^{-2} from the metalloporphyrin itself) seems to indicate that, for each monomer, four pyrrole groups were electropolymerized leading thus to a highly cross-linked structure. If the potential scan range is extended to 1.6 V (not shown), an overoxidation of the polypyrrolic chains occurs inducing their chemical transformation and the loss of the electroactivity of the polypyrrole backbone [26]. The resulting modified electrode exhibits two reversible peak systems at $E_{1/2}$=0.98 and 1.14 V attributed to the two successive one-electron oxidation of poly(ZnTPFPPy) [27] in accordance with the behaviour observed for a non perfluorated poly (ZnTPPy). Although the polypyrrole conductivity was destroyed, the loss of metalloporphyrin electroactivity was estimated to be 28% after 65 scans in the potential range from −1.60 V to 1.20 V illustrating the robustness of the polymeric film and ZnTPFPPy.

As previously described for the electropolymerization of ZnTPFPPy, repeatedly scanning the potential over the range from −1.70 to 1.07 V for MnTPFPPy, results in the slow continuous growth of the cyclic voltammetric peaks of the one-electron reduction of the porphyrin ring and the appearance and growth of its cathodic prepeak reflecting the formation of the polypyrrole skeleton (Fig. 5). Although the functionalization of the Mn porphyrin by one pyrrole group instead of four for Zn porphyrin, allows the electrochemical film formation, the conventional polypyrrole electroactivity was not observed. It should be noted that the intensity of the peak system corresponding to the $Mn^{III/II}$ redox couple, drastically decreases with the growth of the polymer film reflecting a weak charge transfer between the electrode and the polymerized metal sites [24]. Fig. 6 shows the cyclic voltammogram of the resulting electrode transferred with thorough rinsing in CH_3CN+0.1 M TBAP solution free of monomer. Upon negative scanning, three redox systems are observed at $E_{1/2}$=−0.32 V, −1.47 V and −1.88 V. Owing to the similarity in shape and potential values with those recorded for the monomer, these redox processes were attributed to the $Mn^{III/II}$ couple followed by two successive one-electron reduction of the porphyrin ring. The small cathodic prepeak arising at the foot of the first reduction peak of the porphyrin ring disappears on the second scan if the potential scan range is restricted to the negative region corroborating its polypyrrolic origin.

3.3. Potential electrocatalytic properties of polypyrrole films of polyfluorinated Mn(III) porphyrin in the presence of oxygen and benzoic anhydride or H_2O_2 in organic and aqueous media

Since two decades, the development of efficient biomimetic systems for alkane oxidation and alkene epoxidation, for instance to mimic the behavior of cytochrome P_{450}, was mainly based on Fe or Mn porphyrins as catalysts via the generation of high valent metal-oxo intermediate. In this regard, special attention has been devoted to electropolymerized Mn porphyrin films as catalytic electrode materials for biomimetic oxidations with oxygen. Recently, Albin and Bedioui have electrochemically demonstrated the existence of an oxomanganese (V) porphyrin as catalytical active species in the reduction of oxygen and H_2O_2 [28]. Consequently, the electrochemical behavior of the poly MnTPFPPy electrode for the biocatalytic activation of oxygen in the presence of benzoic anhydride was examined in CH_2Cl_2+0.1 M TBAP.

Fig. 7A shows the cyclic voltammograms of a thin poly MnTPFPPy electrode (Γ_{Mn}=7.810^{-10} mol cm^{-2}) recorded in the presence of benzoic anhydride (100 mM) and 1-methylimidazole (5 mM) as axial base (Fig. 7A, a). In the presence of dissolved oxygen, the reduction reaction is illustrated by the

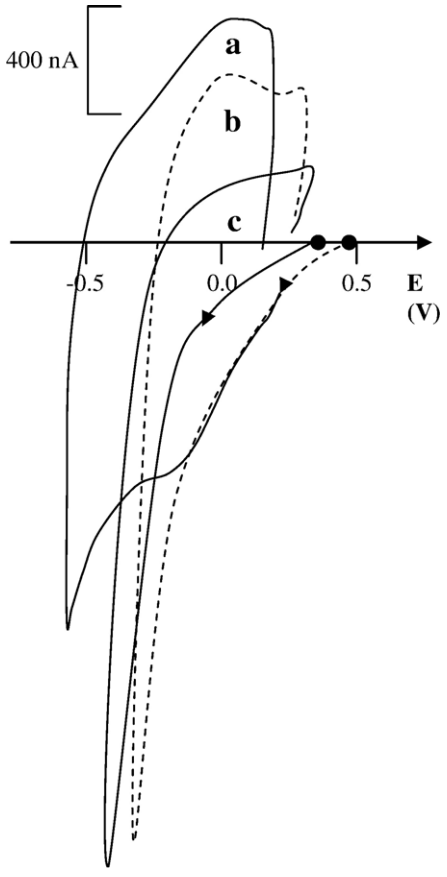

Fig. 8. Cyclic voltammogram at a carbon electrode recorded in a solution of tampon phosphate 0.1 M pH=7 in a presence of 1-methylimidazole (5 mM). Scan rate: 10 mV/s, (a) poly[MnTPPyr] (GC 5 mm) without O_2 and H_2O_2, (b) poly[MnTPPyr] (GC 5 mm) in presence of O_2 and H_2O_2 (1 mM), (c) bare electrode (GC 5 mm) in presence of O_2 and H_2O_2 (1 mM).

increase in the cathodic peak current intensity of the $Mn^{III/II}$ couple (Fig. 7A, b). In comparison with the bare glassy carbon electrode (Fig. 7A c), a strong catalytic wave is observed at less negative potential. This phenomenon was attributed to the activation of oxygen via the formation of high valent manganese oxo-porphyrin species ($Mn^{V}=O$). This chemically generated species are immediately reduced into Mn^{II} porphyrin at the potential value corresponding to the Mn^{III} reduction. To corroborate the activator role of benzoic anhydride on the electrocatalytic activity of the poly Mn porphyrin film, cyclic voltamograms were collected in aerated CH_2Cl_2 with and without benzoic anhydride (Fig. 7B). It clearly appears that the addition benzoic anhydride induces a marked enhancement of the cathodic wave in the presence of oxygen (Fig. 7B, b). This confirms that the observed catalytic phenomenon is not due to the mediated reduction of oxygen.

Since the generation of $Mn^{V}=O$ in aqueous media was reported in the reaction of Mn(III) porphyrin with H_2O_2 or oxygen in the presence of anhydride [28,29], the potential electrocatalytic properties of the poly MnTPFPPy electrode towards the detection of H_2O_2 in the presence of oxygen were investigated by cyclic voltammetry in phosphate buffer 0.1 M (pH 7). Under argon and without H_2O_2, the modified electrode exhibits a reversible $Mn^{III/II}$ peak system at −0.17 V (Fig. 8a). It should be noted that an axial base (1-methylimidazole) was added to observe a well-defined $Mn^{III/II}$ redox process in water. As expected, in the presence of O_2 and H_2O_2, a strong cathodic current appears reflecting the electrochemical reduction of the chemically generated $Mn^{V}=O$ species (Fig. 8b). Compared to the electrochemical behavior of a bare electrode in the presence of O_2 and H_2O_2, these preliminary experiments clearly indicate the catalytic reduction of H_2O_2 by the poly MnTPFPPy electrode at a potential of −0.20 V corresponding to the reduction potential of the $Mn^{III/II}$ redox process (Fig. 8b,c).

4. Conclusion

In this report, we have described the synthesis of new polyfluorinated Zn(II) and Mn(III) porphyrins and their electrochemical characterization, highlighting the marked influence of polyfluorophenyl substituting groups. The electro-oxidation of such metalloporphyrins functionalized by one or four pyrrole groups leads to the successful electrogeneration of polypyrrole films with retention of the electrochemical behaviour of the polyfluorinated Zn(II) and Mn(III) porphyrins. Owing to the potential catalytic properties of such polymerized units associated with the advantages conferred by the electrochemical addressing, it is expected that this approach will be a convenient way for the elaboration of new oxidase-based biosensors involving a reductive detection of H_2O_2.

References

[1] S. Cosnier, Anal. Bioanal. Chem. 377 (2003) 507.
[2] K.M. Kadish, K.M. Smith, R. Guilard (Eds.), The Porphyrin Handbook, Applications: Past, Present and Future, vol. 6, Academic Press, London, 2000.
[3] M. Biegsaga, K. Pyrzynska, M. Trojanowicz, Talanta 51 (2000) 209.
[4] F. Bedioui, J. Devynck, Acc. Chem. Res. 28 (1995) 30.
[5] M.A. Carvalho de Medeiros, S. Cosnier, A. Deronzier, J.-C. Moutet, Inorg. Chem. 35 (1996) 2659.
[6] F. Vilchez-Aguado, S. Gutierrez-Granados, S. Sucar-Succar, C. Bied-Charreton, F. Bedioui, New J. Chem. 21 (1997) 1009.
[7] S. Cosnier, A. Walter, F.-P. Montforts, J. Porphyr. Phthalocyanines 2 (1998) 39.
[8] E. Bruti, M. Giannetto, G. Mori, R. Seeber, Electroanalysis 11 (1999) 565.
[9] S. Cosnier, C. Gondran, R. Wessel, F.P. Monforts, M. Wedel, J. Electroanal. Chem. 488 (2000) 83.
[10] M. Wedel, A. Walter, F.P. Monforts, Eur. J. Org. Chem. (2001) 1681.
[11] S. Griveau, F. Bedioui, Electroanalysis 1 (2001) 13.
[12] N. Diab, W. Schuhmann, Electrochim. Acta 47 (2001) 265.
[13] S. Cosnier, C. Gondran, K. Gorgy, R. Wessel, F.-P. Montforts, M. Wedel, Electrochem. Com. 4 (2002) 426.
[14] A. Goux, F. Bedioui, L. Robbiola, M. Pontié, Electroanalysis 15 (2003) 969.
[15] F. Armijo, M. Goya, Y. Gimeno, M. Arévalo, M. Aguirre, A. Creus, Electrochem. Commun. 8 (2006) 779.
[16] P. Battioni, J.P. Renaud, J.F. Bartoli, M. Reina-Artiles, D. Mansuy, J. Am. Chem. Soc. 110 (1988) 8462.
[17] P.E. Ellis Jr., J.E. Lyons, J. Chem. Soc. Chem. Commun. (1989) 1189.
[18] F. Ojima, N. Kobayashi, T. Osa, Bull. Chem. Soc. Jpn. 63 (1990) 1374.
[19] T. Takeuchi, H.B. Gray, W.A. Goddard, J. Am. Chem. Soc. 116 (1994) 9730.
[20] H. Carpio, E. Galeazzi, R. Greenhouse, A. Guzman, E. Velarde, Y. Antonio, F. Franco, A. Leon, V. Perez, R. Salas, D. Valdes, J. Ackrell, D. Cho, P. Gallegra, O. Halpern, R. Koehler, M.L. Maddox, J.M. Muchouwski, A. Prince, D. Tegg, T.C. Thurber, A.R. Van Horn, D. Wren, Can. J. Chem. 60 (1982) 2295.
[21] K.M. Kadish, C. Aroullo-MaAdams, B.C. Han, M.M. Franzen, J. Am. Chem. Soc. 112 (1990) 8364.
[22] K.M. Kadish, Phys. Bioinorg. Chem. Ser. 34 (1986) 435.
[23] G. Bidan, Sens. Actuators B 6 (1992) 45.
[24] G. Cauquis, S. Cosnier, A. Deronzier, B. Galland, D. Limosin, J.C. Moutet, J. Bizot, D. Deprez, J.P. Pulicani, J. Electroanal. Chem. 352 (1993) 181.
[25] S.E. Creager, R.W. Murray, Inorg. Chem. 26 (1987) 2612.
[26] S. Cosnier, A. Deronzier, J.-F. Roland, J. Electroanal. Chem. 285 (1990) 133.
[27] A. Deronzier, R. Devaux, D. Limosin, J.-M. Latour, J. Electroanal. Chem. 324 (1992) 325.
[28] V. Albin, F. Bedioui, Electrochem. Com. 5 (2003) 129.
[29] W. Nam, I. Kim, M.H. Lim, H.J. Choi, J.S. Lee, H.G. Jang, Chem. Eur. J. 8 (2002) 2067.